Journal of Integrative Agriculture 2016, 15(6): 1256–1266

Available online at www.sciencedirect.com

ScienceDirect

RESEARCH ARTICLE

Combining gas exchange and chlorophyll *a* fluorescence measurements to analyze the photosynthetic activity of drip-irrigated cotton under different soil water deficits

LUO Hong-hai[1*], Tsimilli-michael Merope[2*], ZHANG Ya-li[1], ZHANG Wang-feng[1]

[1] *Key Laboratory of Oasis Ecology Agriculture, Xinjiang Production and Construction Group, Shihezi University, Shihezi 832003, P.R.China*

[2] *Bioenergetics Laboratory, University of Geneva, Jussy-Geneva CH-1254, Switzerland*

Abstract

Gas exchange and chlorophyll *a* fluorescence were measured to study the effects of soil water deficit (75, 60 and 45% of field capacity, FC) on the photosynthetic activity of drip-irrigated cotton under field conditions. At light intensities above 1 200 μmol m^{-2} s^{-1}, leaf net photosynthetic rate (P_n) at 60 and 45% FC was 0.75 and 0.45 times respectively than that of 75% FC. The chlorophyll content, leaf water potential and yield decreased as soil water deficit decreased. Fiber length was significantly lower at 45% FC than at 75% FC. The actual quantum yield of the photosystem II (PSII) primary photochemistry and the photochemical quenching were significantly greater at 60% FC than at 75% FC. The electron transport rate and non-photochemical quenching at 45% FC were 0.91 and 1.29 times than those at 75% FC, respectively. The amplitudes of the K- and L-bands were higher at 45% FC than at 60% FC. As soil water content decreased, active PSII reaction centers per chlorophyll decreased, functional PSII antenna size increased, and energetic connectivity between PSII units decreased. Electron flow from plastoquinol to the PSI end electron acceptors was significantly lower at 45% FC than at 75% FC. Similar to the effect on leaf P_n, water deficit reduced the performance index ($PI_{ABS, total}$) in the dark-adapted state. These results suggest that (i) the effect of mild water deficit on photosystem activity was mainly related to processes between plastoquinol and the PSI end electron acceptors, (ii) PSI end electron acceptors were only affected at moderate water deficit, and (iii) $PI_{ABS, total}$ can reliably indicate the effect of water deficit on the energy supply for cotton metabolism.

Keywords: cotton, drought, JIP-test, modulated fluorescence quenching analysis, photosynthetic rate

1. Introduction

Cotton (*Gossipium hirsutum* L.) is one of the most important fiber-producing plants in the world. Soil water deficits represent a primary limitation to cotton productivity (Ennahli and Earl 2005). Increased mechanistic understanding of the effect of water stress on cotton growth could benefit current efforts to breed more drought tolerant cotton cultivars and improve drought resistance through cultivation

Received 2 June, 2015 Accepted 6 January, 2016
LUO Hong-hai, E-mail: luohonghai79@163.com
Correspondence ZHANG Wang-feng, Tel: +86-993-2057326, Fax: +86-993-2057999, E-mail: Zwf_shzu@163.com
* These authors contributed equally to this study.

doi: 10.1016/S2095-3119(15)61270-9

management.

Photosynthesis is one of the most important physiological processes that is inhibited by water deficit (Kaiser 1987; Raines 2011). Stomatal closure, which is considered the earliest response to water deficit, decreases CO_2 availability at the carboxylation site and consequently decreases leaf CO_2-uptake (Chaves 1991). There is an evidence that non-stomatal components of leaf photosynthesis are also affected by water deficit (Quick *et al*. 1992; Long *et al*. 1994). Photosystem II (PSII) is a photosynthetic component that is highly sensitive to stress conditions; therefore, analysis of PSII function is very important for studying stress effects in plants (Strasser *et al*. 2004; Stirbet and Govindjee 2011). Water deficit can damage the oxygen-evolving system (Chen and Hsu 1995), which concomitantly decreases PSII activity. However, it has not yet been clarified whether water deficit causes (i) a uniform decrease in the activity of the oxygen-evolving system in all reaction centers (RCs) or (ii) the complete inactivation of only a fraction of RCs. Moreover, because less PSII activity leads to greater PSII excitation pressure, it is of great interest to detect and understand the mechanism that regulates PSII function in water-deficient plants.

Chlorophyll (Chl) *a* fluorescence, which originates from PSII RCs, is usually represented by a fast rise followed by a slow decline when exposed to light (Kautsky curve). Based on modulated fluorescence measurements, fluorescence quenching analysis has been developed, leading to the determination of parameters that can be used to evaluate both the structural differences between dark- and light-adapted states and the photosynthetic performance at the light-adapted state (Schreiber *et al*. 2004). Fast Chl *a* fluorescence transient kinetics, a non-invasive spectroscopic technique, represent an excellent tool for detecting and measuring the effect of photosynthetic inhibitors *in vivo*. A typical Chl fluorescence transient shows a sequence of phases from the initial (F_0) to the maximal (F_m) fluorescence value. These steps are labelled as follows: O [all RCs open], J (2 to 3 millisecond (ms)), I (30 ms), and P (equal to F_m when all RCs are closed) (Strasser *et al*. 2004, 2010). Analysis of the OJIP transients using the JIP-test allows the calculation of a constellation of structural, conformational and functional parameters quantifying PSII behavior (Strasser *et al*. 2004; Stirbet and Govindjee 2011). In recent years, this technique has been widely and successfully applied to study PSII behavior in various photosynthetic organisms under stress conditions that result in the establishment of different physiological states (Strasser *et al*. 2004; Chen *et al*. 2015).

This study examined the effect of soil water deficit on the photosynthetic activity of cotton plants grown in the field with plastic film mulch and drip irrigation. Comparisons of photosynthetic activity were carried out at the full boll stage to determine the influence of a long-term water deficit that was applied during the most drought-sensitive stages of development. The photosynthetic light response was measured and compared with cotton yield components and fiber quality. Two methods of fluorescence analysis (fluorescence quenching analysis under steady net photosynthetic rates (P_n) and the JIP-test in the dark-adapted state) were used to identify and evaluate the factors that determine the energy supply for cotton metabolism. The results of this study could be used to identify the best irrigation practices for cotton grown with plastic film mulch and drip irrigation.

2. Results

2.1. Yield components and fiber quality

Boll number, seed cotton yield and lint yield decreased significantly in the order of 75% FC>60% FC>45% FC (Table 1). There was no significant difference in boll weight between 60 and 75% FC; however, boll weights in both treatments were significantly greater than those at 45% FC. The lint percentages at 45 and 60% FC were significantly lower than those at 75% FC. This suggests that the high lint yield at 75% FC was because of the large number of bolls per unit area with high lint percentage.

Water deficit had relatively little effect on cotton fiber quality. The fiber length and fiber strength at 60% FC were greater than those at 45 and 75% FC. The only significant differences were as follows: (i) fiber length was lower at 45% FC than at either 60 or 75% FC and (ii) fiber strength was lower at 45% FC than at 60% FC.

2.2. Chlorophyll content and leaf water potential

Both total Chl content per unit leaf area and midday leaf

Table 1 Yield and fiber quality of cotton grown at different field capacities (FC)

FC (%)	Yield and yield components					Fiber quality		
	Boll number per plant	Boll weight (g)	Lint percentage (%)	Seed cotton yield (kg ha^{-1})	Lint cotton yield (kg ha^{-1})	Length (mm)	Strength (cN tex^{-1})	Micronaire
75	6.6±0.5 a	5.4±0.3 a	41.6±0.1 a	5476±107 a	2278±68 a	29.4±1.7 a	33.5±2.4 ab	4.7±0.1 a
60	4.6±0.4 b	5.3±0.1 a	40.8±0.1 b	4176±109 b	1700±80 b	30.5±0.9 a	34.7±1.6 a	4.8±0.1 a
45	2.6±0.5 c	3.8±0.3 b	40.7±0.1 b	2358±124 c	960±88 c	27.7±1.4 b	31.9±3.3 b	4.9±0.3 a

Values are means±SD. Means within a column followed by a different letter are significantly different (P<0.05). The same as below.

water potential decreased significantly in the order of 75% FC>60% FC>45% FC (Table 2). The decreases were linear (Chl content, R^2=0.9992; leaf water potential, R^2=0.9938). Total chlorophyll content at 60 and 45% FC was 0.93 and 0.85 times respectively than that at 75% FC, respectively. Leaf water potential at 60 and 45% FC was 1.40 and 1.95 times respectively than that at 75% FC, respectively.

2.3. Photosynthetic rates

The P_n rates at >300 μmol photosynthetic photon flux density (PPFD) m^{-2} s^{-1} decreased as water deficit increased (Fig. 1). At 2 000 μmol PPFD m^{-2} s^{-1} (almost complete saturation), the P_n at 60 and 45% FC was approximately 0.75 and 0.45 times greater than that at 75% FC, respectively. The same proportions were observed at as low as 1 200 μmol PPFD m^{-2} s^{-1} (including (1 469±80) μmol PPFD m^{-2} s^{-1}, the PPFD value at which modulated fluorescence was measured in the light-adapted state). Between 500 and 1 200 μmol PPFD m^{-2} s^{-1}, the P_n at 60 and 45% FC was 0.90 and 0.67 times greater than that at 75% FC, respectively. At <300 μmol PPFD m^{-2} s^{-1}, there was no significant difference in P_n between the treatments.

2.4. Fluorescence quenching under steady-state photosynthesis

Neither the actual quantum yield of PSII primary photochemistry ($\varphi P_o'$) nor relative electron transport rates (ETR) reflected changes in PPFD and time of day (Fig. 2). It should be also noted that care was taken to ensure that three soil water treatments were investigated in an alternate way in the course of the experiment.

Table 3 presents the fluorescence quenching analysis depicted in Fig. 2. There were no significant differences in the dark-adapted state fluorescence parameters between the three treatments. However, all nine parameters of light-adapted state were greater at 60% FC than at 75% FC. The average $\varphi P_o'$ and photochemical quenching (q_P) at 60% FC was 1.07 and 1.05 times greater than those at 75% FC, respectively. In contrast, average $\varphi P_o'$ and q_P at 45% FC was 0.91 and 0.95 times greater than those at 75% FC, respectively. This suggests that the 60% FC was the optimal and the 45% FC was worse than the 75% FC in terms of energy conservation.

Table 2 Total chlorophyll (Chl) content per unit leaf area (mg dm^{-2}) and leaf water potential in cotton grown at different FCs

FC (%)	Total Chl per leaf area (mg dm^{-2})	Midday leaf water potential (MPa)
75	6.34±0.12 a	–2.03±0.07 a
60	5.87±0.11 b	–2.86±0.23 b
45	5.35±0.18 c	–3.95±0.24 c

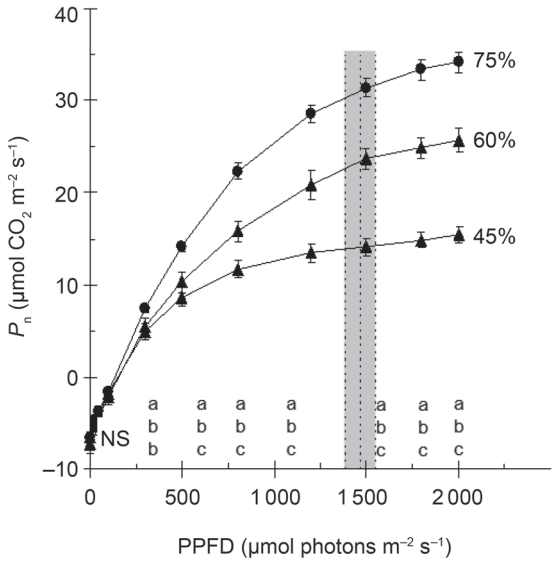

Fig. 1 The light response curves of net CO_2 assimilation (P_n) by leaves from cotton plants grown at 75 (circles), 60 (triangles) and 45% (diamonds) of field capacity. The P_n values represent means±SD of four independent measurements. The photosynthetic photon flux density (PPFD) range marked (1 469±80) μmol photons m^{-2} s^{-1}, refers to the means±SD of the PPFD values under which the light-adapted states were established for modulated fluorescence analysis (Fig. 3). Different lowercase letters above the *x*-axis indicate significant (P<0.05) differences among the treatments. NS, no significant difference. The same as below.

Concerning ETR, non-photochemical quenching (NPQ), and the approximated non-photochemical quenching coefficient (q_N) values, the differences between 60 and 75% FC were not significant. In contrast, the ETR, NPQ and q_N at 45% FC was 0.91, 1.29 and 1.14 times greater than those at 75% FC, respectively (P<0.05).

2.5. OJIP fluorescence transients of dark-adapted leaves

Fig. 3 shows the averages of the raw fluorescence transients, plotted on logarithmic time scale from 20 ms to 1 s. The steps O, J, I, and P are indicated. The fluorescence values are expressed as F_t/F_0 so that differences in F_0 values do not interfere with the other differences. The average F_0 intensity increased as soil water content decreased. The three transients had a typical OJIP shape, with small differences between them (Fig. 3). In order to reveal hidden differences, the three transients were expressed and plotted in Fig. 4-A–C as kinetics of different expressions of relative variable fluorescence. This method of data processing facilitated the comparison of the normalized transients.

There were two clearly distinct bands in the kinetics of

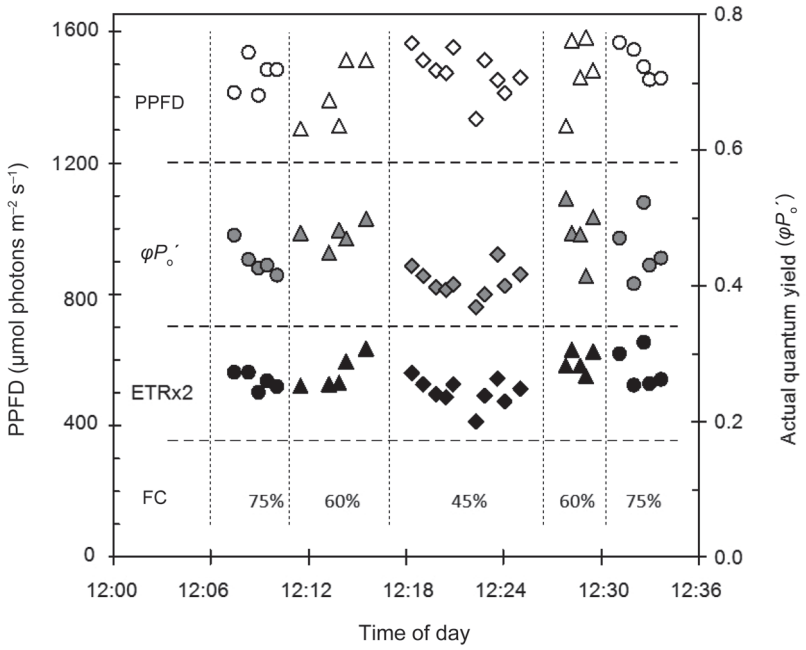

Fig. 2 The sunlight PPFD (open symbols) under which the light-adapted states were established (left vertical axis) and the corresponding actual quantum yield of primary photochemistry (grey symbols; right vertical axis) and relative electron transport rate (ETR; black symbols; left vertical axis, with ETR multiplied by 2 for clarity) during the experiment (separated by horizontal dashed lines). The modulated fluorescence measurements were conducted at full boll stage on leaves of cotton grown at 75 (circles), 60 (triangles) and 45% (diamonds) of field capacity. FC, field capacity.

Table 3 Fluorescence quenching analysis by modulated fluorescence measurements on leaves of cotton plants grown at different FCs

Fluorescence quenching parameters	75% FC	60% FC	45% FC
Dark-adapted state			
F_0	0.16±0.01 a	0.15±0.01 a	0.16±0.02 a
F_m	0.94±0.04 a	0.97±0.06 a	1.00±0.09 a
φP_o	0.83±0.01 a	0.84±0.01 a	0.84±0.01 a
Light-adapted state			
F_m'	0.54±0.05 ab	0.57±0.06 a	0.51±0.05 b
F_s'	0.30±0.02 a	0.30±0.03 a	0.30±0.03 a
$\varphi P_o'$	0.45±0.04 a	0.48±0.03 b	0.41±0.02 c
ETR	276±24 a	289±22 a	251±21 b
$\approx\varphi P_o'$	0.71±0.03 ab	0.73 ± 0.03 a	0.68±0.03 b
$\approx q_P$	0.63±0.03 b	0.66±0.04 a	0.59±0.03 c
$\approx^* F_0'$	0.14±0.01 a	0.14±0.01 a	0.14±0.01 a
$\approx^* \varphi P_o'$	0.74±0.02 ab	0.75±0.02 a	0.73±0.02 b
$\approx^* q_P$	0.60±0.03 a	0.63±0.04 b	0.56±0.02 c
Comparison of light- and dark-adapted states			
NPQ	0.74±0.14 b	0.72±0.18 b	0.96±0.18 a
$\approx q_N$	0.51±0.06 b	0.49±0.08 b	0.58±0.05 a
$\approx^* q_N$	0.49±0.05 b	0.47±0.07 b	0.55±0.05 a

[1] F_0, the minimal fluorescence intensities; F_m, the maximal fluorescence intensities; φP_o, the maximum quantum yield of primary photochemistry; F_m', the maximal fluorescence intensities; F_s', actua fluorescence intensities; $\varphi P_o'$, approximated maximum quantum yield of primary photochemistry; ETR, electron transport rate; q_P, coefficient of photochemical quenching; q_N, coefficient of nonphotochemical quenching of Chl *a* fluorescence; *, approximated.

.

$\Delta[(F_m-F_0)/(F_m-F_0)]=\Delta V_t$, one from 20 μs to 20 ms and the other from 20 to 200 ms (Fig. 4-A). The ΔV_t between 60 and 75% FC was present in the O–I band only. In contrast, the ΔV_t between 45 and 75% FC was present in the I–P band. Furthermore, the I–P band was more pronounced than the O–J band, which, in turn, was more pronounced than the ΔV_t between 60 and 75% FC.

When focusing on the differences in the O–J phase of

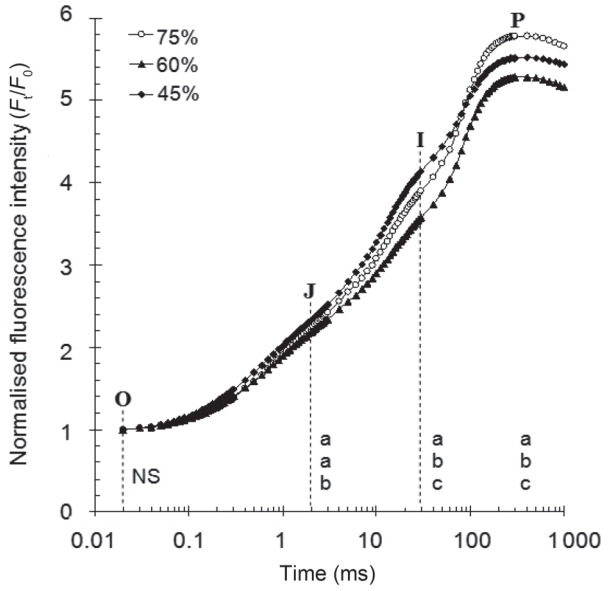

Fig. 3 The polyphasic chlorophyll *a* fluorescence transients (OIJP) of dark-adapted leaves of cotton grown at 75 (circles), 60 (triangles) and 45% (diamonds) of field capacity.

the transients, a positive K-band in the kinetics of $\Delta[(F_t-F_0)/(F_J-F_0)]=W_t$ was observed (Fig. 4-B). The K-band appeared at the same time, 500 μs, at both 45% FC and 60% FC; however, the amplitude of the band was higher at 45% FC than at 60% FC.

Fig. 4-C shows different kinetics in the 20–300 μs time range, $\Delta[(F_t-F_o)/(F_{300\ ms}-F_o)]$. A positive L-band, at about 170 μs, was observed at both 60 and 45% FC. This indicates a decrease in energetic connectivity between PSII units compared with 75% FC (Strasser *et al*. 2004, 2007). The decrease was more pronounced at 45% FC than at 60% FC.

Fig. 4-D shows two normalizations of the I–P portion of the transients. The inserted figure, which is also normalized, shows differences in the relative amplitude of the I–P phase between the three treatments. There was no difference in amplitude between 75 and 60% FC; however, the amplitude was reduced at 45% FC.

2.6. JIP-test parameters of dark-adapted leaves

In Fig. 5-A, Trapping (TR_0)/Absorption (ABS) and electron transport between PSII and PSI (ET_0)/ABS, which refer to processes between exciton trapping and PQ reduction, were slightly less at 60% FC than at 75% FC. There was no significant difference in TR_0/ABS and ET_o/ABS between 45 and 75% FC. In comparison, there was no significant difference between 75 and 60% FC in either reduction of PSI end electron acceptors (RE_0)/ABS or RE_0/ET_0, which refer to electron flow from PQH_2 to the PSI end electron acceptors. The RE_0/ABS and E_0/ET_0 of 45% FC were significantly lower than those at 75 and 60% FC.

The reaction center (RC)/ABS decreased as water deficit decreased (Fig. 5-A). This was equivalent to the increase in ABS/RC in Fig. 5-B. In general, an increase in ABS/RC means either (i) inactivation of a fraction of the RCs (i.e., increase in the apparent antenna size), in which case TR_0/RC is not affected, or (ii) an increase in functional antenna size, in which case TR_0/RC also increases provided the PSII de-excitation rate constants do not change. These results suggest that the second explanation is more likely because TR_0/RC closely followed the increase in ABS/RC (Fig. 5-B), which was equivalent to ET_0/ABS stability (Fig. 5-A).

Similar to ABS/RC, RE_0/RC was greater at 60% FC than at 75% FC (Fig. 5-B). In contrast, ABS/RC at 45% FC was less than that at 75% FC. This was in accordance with changes in EC_0/ABS (Fig. 5-A) and EC_0/RC (Fig. 5-B). The stability of EC_0/RC indicated that the decrease in EC_0/ABS at 60% FC was solely due to the decrease in RC/ABS, whereas the additional decline in RE_0/ABS at 45% FC was predominantly due to the decrease in EC_0/RC.

2.7. Comparison of photosynthetic parameters derived by three approaches

Fig. 6 shows the effects of water deficit on photosynthetic parameters derived by the three experimental approaches. The parameters derived by fluorescence quenching analysis of modulated fluorescence data (represented by ETR in Fig. 6) exhibited a very different behaviour to P_n as the soil water content decreased from 75 to 45% FC, even though fluorescence and P_n were both determined at a light-adapted state established with identical PPFD. The PI_{ABS} and PI_{total} declined by similar proportions at 60% FC; however, they deviated from each other at 45% FC (Fig. 6). This supports the previous observation that the processes related to electron transport from PQH_2 to the PSI end electron acceptors were affected only when the water deficit decreased from 60 to 45% FC.

3. Discussion

3.1. The different mechanisms in the reduction of photosynthetic activity of cotton under different water deficits

The P_n (from about 1 200 μmol m^{-2} s^{-1} up to saturation), chlorophyll content, leaf water potential, cotton seed yield, and lint yield all decreased as soil water content decreased (Fig. 1, Tables 1 and 2). This suggests that soil deficit during the flowering and boll-setting stages can influence the leaf photosynthetic capacity and yield. However, fiber length and fiber strength at 60% FC were greater than those at 45 and 75% FC. This may be because a mild water deficit slightly

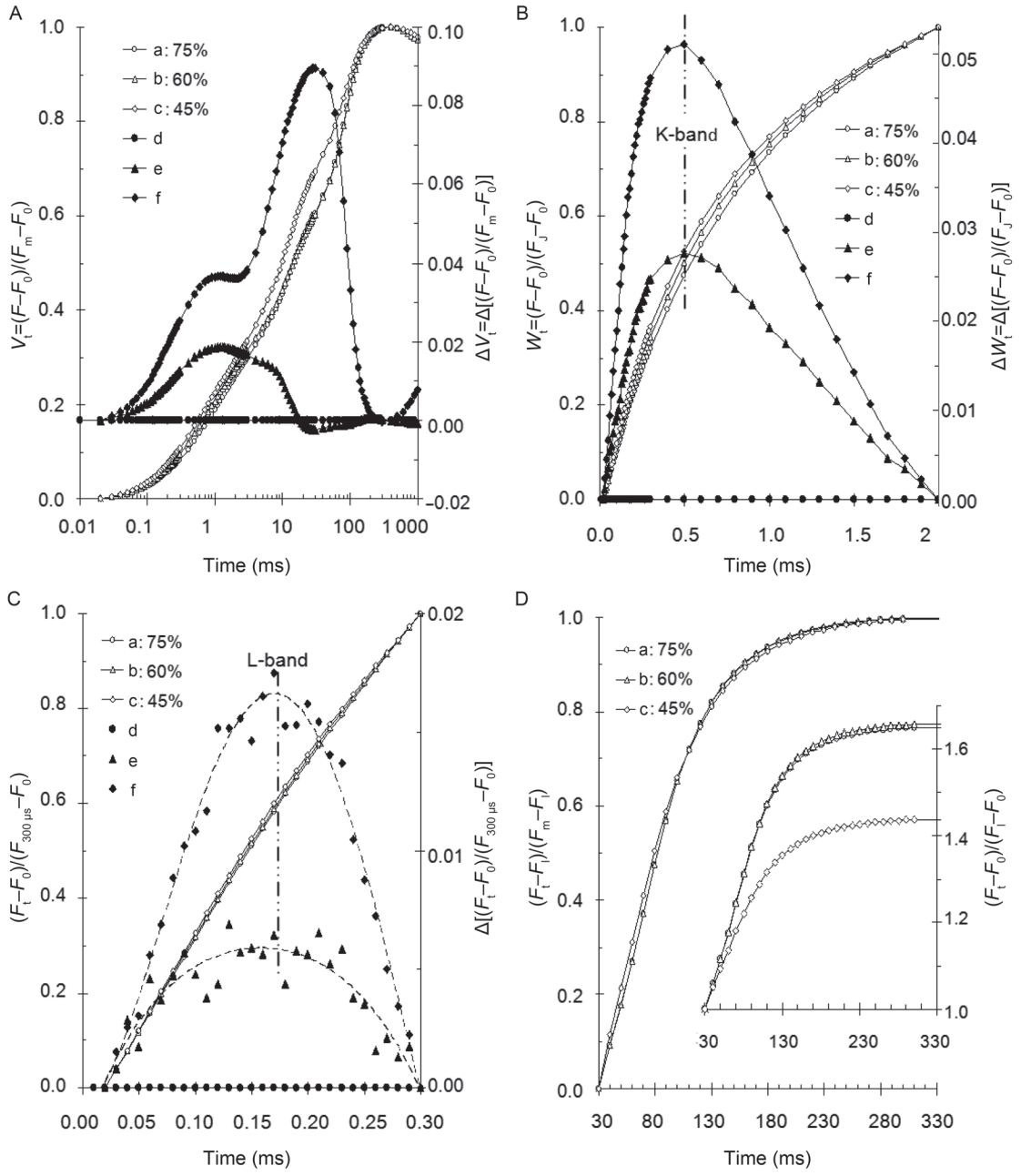

Fig. 4 The chlorophyll *a* fluorescence kinetics (F_t) of Fig. 3 (a, b and c, 75, 60 and 45% of field capacity respectively) are presented as the kinetics of different expressions of relative variable fluorescence: between F_0 and F_m: $V_t=(F_t–F_0)/(F_m–F_0)$ (A); between F_0 and F_J: $W_t=(F_t–F_0)/(F_J–F_0)$ (B); between F_0 and $F_{300\ \mu s}$: $(F_t–F_0)/(F_{300\ \mu s}–F_0)$ (C); between F_I and F_m: $(F_t–F_I)/(F_m–F_I)$ (D) and, in the insert, between F_0 and F_I: $(F_t–F_0)/(F_I–F_0)$. In each of the plots, d, e and f, kinetics of different expressions of relative variable fluorescence (RVF), are also presented (right vertical axis); the [RVF] kinetics result (as indicated) by subtracting the RVF kinetics of the control (A) from each of the three RVF kinetics. The K- and L-bands are clearly revealed in plots B and C, respectively.

increased the cellulose accumulation rate (Jiao 2014).

A key question is whether P_n suppression is due to a decrease in PSII activity. According to Chen and Hsu (1995), water deficit caused PSII activity to decline by damaging the oxygen-evolving system. In contrast, Genty *et al*. (1987) reported that PSII photochemistry is unaffected by drought in a controlled environment. Comparison of the light response curves in Fig. 1 with the fluorescence quenching analysis (Table 3, Fig. 2) clearly demonstrates that the effect of water deficit on ETR differed widely from its effect on P_n. The leaf P_n decreased substantially more than ETR at 45% FC (Fig. 2). This strongly suggests that water deficit affects processes after PQH_2. There was no difference in RE_0/ET_0 between 60 and 75% FC. This indicates that the electron

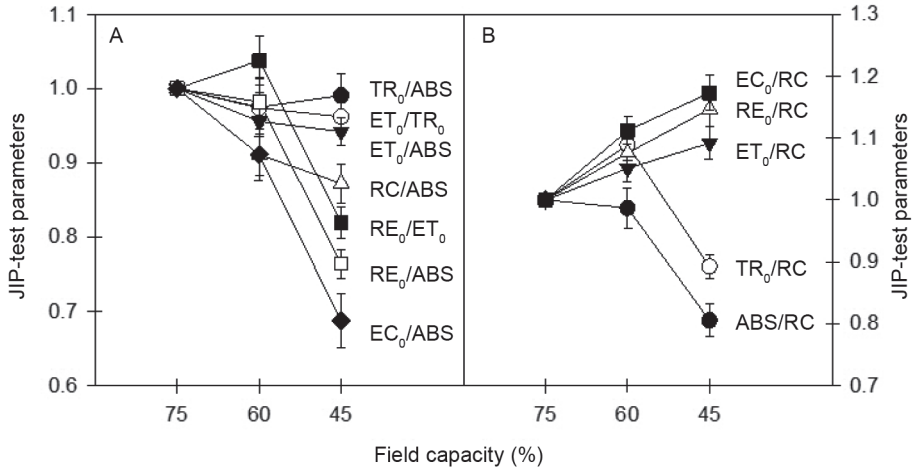

Fig. 5 Photosynthetic parameters (at time zero, all reaction centres (RCs) open) derived by the JIP-test from the fluorescence transients of dark-adapted leaves of cotton plants as affected by soil water content. The parameters were presented relative to their control values (75% of field capacity). Error bars represent the means±SD. The same as below.

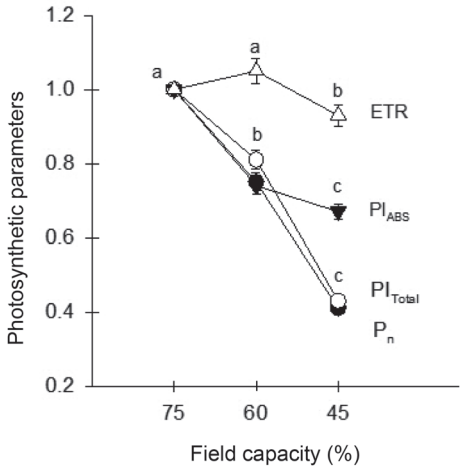

Fig. 6 Photosynthetic parameters of cotton leaves at full boll stage as affected by soil water content. The values are presented relative to the control (75% of field capacity). The parameters were obtained using three experimental approaches: P_n, fluorescence quenching analysis under steady P_n and the JIP-test at the dark-adapted state. For each variable, values with different letters are significantly different (P<0.05).

flow was still proceeding normally from PQH_2 to the PSI end electron acceptors at 60% FC. This means that when the photosynthetic system transfers from the dark-adapted to the light-adapted state, the over-reduction of the intersystem electron transport chain was the same at 60% FC as at 75% FC. The capacity of the end electron acceptor pool was smaller at 45% FC than at 75% FC. Therefore, when the photosynthetic system transferred from the dark-adapted state to the light-adapted state, the increase of dissipation from the antennae was wider at 45% FC than that at 75% FC. This led to greater NPQ, which is an efficient photoprotection mechanism (Demmig-Adams 1990; Jiang *et al*. 2001).

3.2. The JIP-test is a powerful tool to estimate the photosynthetic activity of cotton to water deficit

A positive K-band reflects an electron donation from internal electron donors competing with the oxygen evolving system (Strasser *et al*. 2004, 2007). The amplitude of the K-band was higher at 45% FC than at 60% FC (Fig. 4-B). This indicates that water deficit can reduce inactivation of the oxygen evolving complexes oxygen evolving complex. The L-band revealed differences in energetic connectivity among PSII units (Strasser *et al*. 2004, 2007). The energetic connectivity among PSII units declined as water deficit increased (Fig. 4-C). It was expected that water deficit could reduce the utilization efficiency of excitation energy and the stability of photosynthetic systems. However, there was no significant difference between the three treatments in the conformation of the electron transfer pathway, i.e., the Michaelis-Menten constants of the electron transfer pathway from PQH_2 to NADPH (Fig. 4-D). This interpretation was verified and also quantified by the JIP-test, which showed a clear distinction between the RE_0/ABS and the quantum yield of electron transport from Q_A to the PSI electron acceptors (Zhang *et al*. 2013). The ratios RE_0/RC, ABS/RC and EC_0/RC declined by similar proportions between 75 and 60% FC. However, they diverged when soil water content declined to 45% FC (Fig. 5-B). This suggests that (i) the processes from PQH_2 to the PSI end electron acceptors were only affected when the soil water content decreased from 60 to 45% FC and (ii) the main effect of moderate deficit on photosystem

activity was the decrease in the PSI end electron acceptors.

The performance index (PI_{ABS}) combines the response of PSII to (i) photochemical and non-photochemical properties and (ii) the density of active RCs per chlorophyll. The PI_{ABS} may be the most sensitive, experimentally-derived parameter to stress (Demetriou *et al*. 2007). As soil water content decreased from 75 to 45% FC, the decrease in $PI_{ABS, total}$ was similar to the decrease in P_n (at >1 200 mmol m^{-2} s^{-1}) (Fig. 6). This means that PI_{ABS} can be reliably used as an indicator of the effect of water deficit on the CO_2 assimilation rate. It could be argued that this is unreasonable because CO_2 assimilation rate can also be regulated by modifications after Rubisco that are not detected by measurements at the dark-adapted state, i.e., when Rubisco is inactive. However, it should be taken into consideration that two types of adaptation are being dealt with in this experiment. The plants were adapting not only to water deficit but also to alternating dark and light conditions, with the latter established under PPFD values above 1 200 mmol m^{-2} s^{-1} for about six hours (11:15 to 17:15; see Fig. 2). The $PI_{ABS, total}$ reflects both types of adaptations (i.e., adaptations to water deficit and to diurnal changes in light). Thus, even though it is measured in the dark state, $PI_{ABS, total}$ is a measure of potential photosynthetic activity under midday light conditions.

4. Conclusion

The leaf P_n, chlorophyll content, water potential, and yield decreased as soil water content decreased. Fiber length was significantly lower at 45% FC than at 75% FC. The ETR was the same or only slightly lower at 60 and 45% FC than at 75% FC. This implies that a reduction in soil water deficit affects processes after PQH_2. Water deficit caused a decrease in PSII active RCs per chlorophyll, an increase in functional PSII-antenna size, and a decrease in energetic connectivity among PSII units. The electron flow from plastoquinol to the PSI end electron acceptors decreased at 45% FC but not at 60% FC. The decreases in $PI_{ABS, total}$ as water deficit increased were similar to those observed for P_n. This indicates that $PI_{ABS, total}$ can be used to indicate the effects of soil water deficit on the energy supply for cotton metabolism and yield.

5. Materials and methods

5.1. Experimental site and treatments

This study took place as part of a larger field experiment that was conducted in 2006 at the Shihezi University Research Station in the Xinjiang Uyghur Autonomous Region, China (45°19′N, 86°03′E). Cotton (*cv*. Xinluzao 13) was grown in nine identical plots (9 m×7 m). Plastic film was installed to a depth of 1.5 m around the edge of each plot to prevent lateral water movement. The soil was fully irrigated before winter to increase soil water content in the deep soil layer.

The cotton was sown at 240 000 plants ha^{-1} on 24 April. The row spacing alternated between 30 and 70 cm. There was 10 cm between plants within a row. Before sowing, the 70 cm wide rows were mulched with plastic film. Drip tapes with emitters were installed under the mulch. The cotton was drip-irrigated after sowing to ensure germination. Afterwards, no water was applied until the full bud stage (19 June; 52 days after emergence). The amount of rainfall was 81.8 mm and evapotranspiration was 1 400 mm during the growing season. Fertilizer (240 kg N ha^{-1} and 172.5 kg P_2O_5 ha^{-1}) was applied before sowing. Potassium fertilizer was not applied because of the high K_2O content of the soil. Pest control was carried out according to local practices.

A randomized complete block design was used with three replicates. The experimental treatments, which began when the cotton reached the full-bud stage, comprised three levels of water deficit: ~75, ~60 and ~45% of field capacity (FC, averaged over the 0–60 cm depth). These treatments have been classified as well-watered (control), mild drought and moderate drought, respectively (Hsiao 1973). Soil water content in the 0–20, 20–40 and 40–60 cm soil depths was measured every other day using time domain reflectometry (Trime-T_3, Germany). A set of three stainless steel waveguides (20 cm long, 3.0 mm diameter) were buried vertically in each soil layer. The plots were drip irrigated every 6 d to maintain the soil water content within the designed limits for each treatment. The total amounts of irrigation water were 5 400, 3 600 and 1 800 mm at 75, 60 and 45% FC, respectively.

5.2. Determination of chlorophyll content, leaf water status, yield, and fiber quality

Leaf total chlorophyll content, leaf relative water content and leaf water potential were determined at the full boll stage (30 July, 92 d after emergence), and fluorescence and CO_2 assimilation rate measurements were also conducted. Chlorophyll was extracted by grinding leaf discs (1 cm diameter) in 80% (v/v) acetone/water. The chlorophyll content of the extracts was determined spectrophotometrically.

Leaf water potential was measured with an SKPM 1400 pressure chamber (Skye, UK) between 10:00 and 12:00 a.m. The leaf lamina was enclosed in the chamber and subjected to increasing pressure from a compressed nitrogen cylinder until free sap was visible at the petiole outside the chamber.

The following yield and yield components were measured at harvest on 25 September: boll number per plant, boll weight, lint percentage, seed cotton yield, and lint cotton yield. Cotton fiber quality was evaluated by measuring fiber

length, strength and micronaire.

5.3. Light response curves of CO_2 assimilation rate

Net photosynthetic rates (P_n) were measured at the full boll stage (92 d after emergence) at ambient CO_2 (380 μmol CO_2 mol^{-1}), 21% O_2 and temperatures between 32 and 35°C. Photosynthetic light response curves were obtained using the automatic LI-6400 photosynthesis system. Illumination was provided by a red/blue LED source (LI 6400–02B, LI-COR, Lincoln, USA). The leaf P_n was measured after equilibration at each of the 11 applied irradiances. For each treatment, four individual plants were sampled. The measurements were conducted on the 4th leaf from the top of the plant.

5.4. Fluorescence quenching analysis under steady-state photosynthesis

Chlorophyll *a* fluorescence parameters were measured at midday at the full boll stage (92 d after emergence), using a PAM-2100 fluorometer equipped with a fiber optic probe and a 2030-B leaf clip holder (Heinz Walz GmbH, Effeltrich, Germany). The fluorometer settings were: modulation frequency of the light source, 20 kHz; gain, level 4; damping, level 2; and measuring light intensity, level 9. Before dawn, i.e., at the dark-adapted state, the maximal (F_m) and minimal (F_0) fluorescence intensities were determined. The leaves were marked so that they could be measured at the light-adapted state. The steady-state fluorescence intensity (F_s') was measured first, followed by exposure to a saturating light pulse provided by the instrument's halogen source to allow maximum fluorescence intensity F_m' to be determined. The microquantum sensor located on the leaf clip holder recorded the PPFD of sunlight incident to the leaf at the time of F_s' determination. For each treatment, 10 individual plants were sampled and measurements were conducted on the fourth leaf from the top of the plant. The minimal fluorescence intensity at the light-adapted state, F_0', was calculated following both approximations currently used, $F_0' \approx F_0$ (Oxborough and Baker 1997).

The calculated parameters are as follows: (A) For the dark-adapted state, the maximal quantum yield of PSII primary photochemistry (φP_o) equals $F_v/F_m=1-F_0/F_m$. (B) For the light-adapted state, (i) the actual quantum yield of PSII primary photochemistry ($\varphi P_o'$) equals $1-F_s'/F_m'$ (Schreiber 2004); (ii) the relative electron transport rate (ETR) equals FPSII×PAR×K, where, PAR is the photosynthetically active radiation (or PPFD) under which the light-adapted state is established and K is a constant; (iii) the approximated maximum quantum yield of primary photochemistry ($\varphi P_o'$) equals $1-F_0'/F_m'$; (iv) the approximated coefficient of overall q_P equals $(F_m'-F_s')/(F_m'-F_0')$. (C) For the comparison of the light- and dark-adapted states, the nonphotochemical quenching (NPQ) equals $(F_m-F_m')/F_m'$.

5.5. OJIP at the dark-adapted state and the JIP-test

Chlorophyll *a* fluorescence transients were measured with a Handy-Pea fluorimeter (Plant Efficiency Analyser, Hansatech Instruments Ltd., UK). The measurements were made using terminal leaflets of fully expanded leaves at the mid-stem position of 3–4 plants (50 replicates per treatment). The leaves were dark-adapted for 45 min before measurement. The transients were induced by red light (peak at 650 nm, 3 500 μmol m^{-2} s^{-1}) from an array of three light-emitting diodes. The transients were recorded for 1 s with 12-bit resolution. The data acquisition took place every 10 μs from 10 μs to 0.3 ms, every 0.1 ms from 0.3 to 3 ms, every 1 ms from 3 to 30 ms, every 10 ms from 30 to 300 ms, and every 100 ms from 300 ms to 1 s (Strasser and Strasser 1995; Schansker *et al*. 2005).

The OJIP transients were analysed using the JIP-test (Strasser *et al*. 2004; Tsimilli-Michael and Strasser 2013) with Biolyzer software (Laboratory of Bioenergetics, University of Geneva, Switzerland). The following original data were utilized by the JIP-test: the maximal measured fluorescence intensity, F_P, which is equal to F_m because the excitation intensity was high enough to ensure the closure of all RCs; the fluorescence intensity at 20 μs (F_0); the fluorescence intensities at 50 and 300 μs, which are required to calculate the initial slope $M_0=(dV/dt)_0 \cong V_{300\,\mu s}/250$ μs of the relative variable fluorescence kinetics, $V_t=(F_t-F_0)/F_m-F_0$; the fluorescence intensities at 2 ms (F_J) and at 30 ms (F_I); the complementary area (Area) above the fluorescence curve, i.e., the area between the curve, the horizontal line $F=F_m$ and the vertical lines at t=20 ms and at $t=t_{F_m}$.

The JIP-test parameters, all referring to the condition of the sample at time zero (onset of fluorescence induction; all RCs open) are as follows:

(i) The flux ratios or yields, namely, the maximum quantum yield of primary photochemistry ($TR_0/ABS=\varphi P_o=1-F_0/F_m$), the efficiency ($ET_0/TR_0=\psi E_0=1-V_J$) with which a trapped exciton can move an electron into the electron transport chain from Q_A^- to the plastoquinone pool (PQ), the quantum yield of electron transport from Q_A^- to PQ ($ET_0/ABS=\varphi E_0=\varphi P_o\times\psi E_0$), the efficiency of electron transport from reduced plastoquinone (plastoquinol, PQH_2) to the PSI end electron acceptors ($RE_0=ET_0=\delta R_0=(1-V_I)/(1-V_J)$) and the quantum yield of electron transport from Q_A^- to the PSI electron acceptors ($RE_0/ABS=\varphi R_0=\varphi P_o\times\psi E_0\times\delta R_0$).

(ii) The specific energy fluxes (per RC; in arbitrary units): for absorption, $ABS/RC=(M_0/V_J)\times F_m/(F_m-F_0)$; trapping, $TR_0/RC=(M_0/V_J)$; electron transport from Q_A^- to PQ, $ET_0/RC=(M_0/$

V_J)×(1–V_J); and electron transport from Q_A^- to the PSI electron acceptors, $RE_0/RC=(M_0/V_J)\times(1-V_I)$.

(iii) The number of active RCs per absorption, $RC/ABS=(ABS/RC)^{-1}$

(iv) The total electron carriers per RC, $EC_0/RC=Area(F_m-F_0)\equiv(S_m)$

(v) The performance indexes PI_{ABS} and PI_{total}, which are products of terms expressing partial potentials for energy conservation at the sequential energy bifurcations from exciton to PQ reduction and to the reduction of PSI end acceptors, respectively.

$$PI_{ABS}=[RC/ABS]\times[\varphi P_o/(1-\varphi P_o)]\times[\psi E_0/(1-\psi E_0]$$
$$=[RC/ABS]\times[TR_0/(ABS-TR_0)]\times[ET_0/(TR_0-ET_0)]$$
$$PI_{total}=[RC/ABS]\times[\varphi P_o/(1-\varphi P_o)]\times[\psi E_0/(1-\psi E_0]\times[\delta R_0/(1-\delta R_0)]$$
$$=[RC/ABS]\times[TR_0/(ABS-TR_0)]\times[ET_0/(TR_0-ET_0)]\times[RE_0/(ET_0-RE_0)]$$

5.6. Statistical analysis

Analysis of variance was conducted using SPSS ver. 11.0 software. Tukey's procedure was used to test for significant differences between means (P<0.05).

Acknowledgements

This study was supported by the National Natural Science Foundation of China (31401321 and U1203283), the Pairing Program of Shihezi University with Eminent Scholars in Elite Universities (SDJDZ201510) and the Swiss National Science Foundation (200021-116765).

References

Chaves M M. 1991. Effects of water deficits on carbon assimilation. *Journal of Experimental Botany*, **42**, 1–16.

Chen S G, Kang Y, Zhang M, Wang X X, Strasser R J, Zhou B, Qiang S. 2015. Differential sensitivity to the potential bioherbicide tenuazonic acid probed by the JIP-test based on fast chlorophyll fluorescence kinetics. *Environmental and Experimental Botany*, **112**, 1–15.

Chen Y H, Hsu B D. 1995. Effects of dehydration on the electron transport of Chlorella. An *in vivo* fluorescence study. *Photosynthesis Research*, **46**, 295–299.

Demetriou G, Neonaki C, Navakoudis E, Kotzabasis K. 2007. Salt stress impact on the molecular structure and function of the photosynthetic apparatus-theprotective role of polyamines. *Biochimica et Biophysica Acta-Bioenergetics*, **1767**, 272–280.

Demmig-Adams B. 1990. Carotenoids and photoprotection in plant: A role for the xanthophyll zeaxanthin. *Biochimica et Biophysica Acta-Bioenergetics*, **1020**, 1–24.

Ennahli S, Earl H J. 2005. Physiological limitations to photosynthetic carbon assimilation in cotton under water stress. *Crop Science*, **45**, 2374–2382.

Genty B, Briantais J M, Da Silva J B V. 1987. Effects of drought on primary photosynthetic processes of cotton leaves. *Plant Physiology*, **83**, 360–364.

Hsiao T C. 1973. Plant responses to water stress. *Annual Review of Plant Biology*, **24**, 519–570.

Jiang C D, Gao H Y, Zou Q. 2001. Enhanced thermal energy dissipation depending on xanthophyll cycle and D_1 protein turnover in iron-deficient maize leaves under high irradiance. *Photosynthetica*, **39**, 269–274.

Jiao X L. 2014. The effects of non-sufficient irrigation on boll development and fibre quality of cotton. MSc thesis, Xinjiang Agriculture University, China. (in Chinese)

Kaiser W M. 1987. Effects of water deficit on photosynthetic capacity. *Physiologia Plantarum*, **71**, 142–149.

Kitao M, Lei T T. 2007. Circumvention of over-excitation of PSII by maintaining electron transport rate in leaves of four cotton genotypes developed under long-term drought. *Plant Biology*, **9**, 69–76.

Long S P, Humphries S, Falkowski P G. 1994. Photoinhibition of photosynthesis in nature. *Annual Review of Plant Biology*, **45**, 633–662.

Oxborough K, Baker N R. 1997. An instrument capable of imaging chlorophyll a fluorescence from intact leaves at very low irradiance and at cellular and subcellular levels of organization. *Plant*, *Cell and Environment*, **20**, 1473–1483.

Quick W P, Chaves M M, Wendler R, David M, Rodrigues M L, Passaharinho J A, Pereira J S, Adcock M D, Leegood R C, Stitt M. 1992. The effect of water stress on photosynthetic carbon metabolism in four species grown under field conditions. *Plant*, *Cell and Environment*, **15**, 25–35.

Raines C A. 2011. Increasing photosynthetic carbon assimilation in C_3 plant to improve crop yield: Current and future strategies. *Plant Physiology*, **155**, 36–42.

Schansker G, Tóth S Z, Strasser R J. 2005. Methylviologen and dibromothymoquinone treatments of pea leaves reveal the role of photosystem I in the Chl *a* fluorescence rise OJIP. *Biochimica et Biophysica Acta-Bioenergetics*, **1706**, 250–261.

Schreiber U. 2004. Pulse-amplitude modulation (PAM) fluorometry and saturation pulse method: An overview. In: Yunus M, Pathre U, Mohanty P, eds., *Probing Photosynthesis*: *Mechanism*, *Regulation and Adaptation*. Taylor & Francis, London. pp. 279–319.

Stirbet A, Govindjee. 2011. On the relation between the Kautsky effect (chlorophyll *a* fluorescence induction) and photosystem II: Basics and applications of the OJIP fluorescence transient. *Journal of Photochemistry and Photobiology* (B-Biology), **104**, 236–257.

Strasser B J, Strasser R J. 1995. Measuring fast fluorescence transients to address environmental questions: The JIP -test. In: Mathis P, ed., *Photosynthesis: From Light to Biosphere*. Kluwer Academic Publishers, Dodrecht. pp. 977–980.

Strasser R J, Tsimilli-Michael M, Dangre D, Rai M. 2007.

Biophysical phenomics reveals functional building blocks of plants systems biology: A case study for the evaluation of the impact of mycorrhization with piriformospora indica. In: Varma A, Oelmüler R, eds., *Advanced Techniques in Soil Microbiology*, *Soil Biology*. Springer-Verlag, Berlin Heidelberg. pp. 319–341.

Strasser R J, Tsimilli-Michael M, Srivastava A. 2004. Analysis of the chlorophyll a fluorescence transient. In: Papageorgiou G C, Govindjee, eds., *Chlorophyll a Fluorescence*: *Asignature of Photosynthesis. Advances in Photosynthesis and Respiration Series*. Kluwer Academic Publishers, Rotterdam. pp. 321–362.

Strasser R J, Tsimilli-Michael M, Qiang S, Goltsev V. 2010. Simultaneous *in vivo* recording of prompt and delayed fluorescence and 820-nm reflection changes during drying and after rehydration of the resurrection plant Haberlea rhodopensis. *Biochimica et Biophysica Acta-Bioenergetics*, **1797**, 1313–1326.

Tsimilli-Michael M, Strasser R J. 2013. The energy flux theory 35 years later: Formulations and applications. *Photosynthesis Research*, **117**, 289–320.

Zhang Y L, Luo H H, Hu Y Y, Strasser R J, Zhang W F. 2013. Characteristics of photosystem II behavior in cotton (*Gossypium hirsutum* L.) bract and capsule wall. *Journal of Integrative Agriculture*, **12**, 2056–2064.

(Managing editor WANG Ning)